On Species Persistence-Time Distributions

S. Suweis[a], E. Bertuzzo[a], L. Mari[a], I. Rodriguez-Iturbe[b], A. Maritan[c], A. Rinaldo[a,d]

[a]*Laboratory of Ecohydrology (ECHO/IIE/ENAC), Ecole Polytechnique Fédérale Lausanne (EPFL), School of Architecture, Civil and Environmental Engineering (ENAC), 1015 Lausanne, (CH)*
[b]*Department of Civil and Environmental Engineering, Princeton University, Princeton, NJ 08544, (USA)*
[c]*Department of Physics, University of Padua, CNISM and INFN, via Marzolo 9, 35131 Padova (Italy)*
[d]*Dipartimento IMAGE, University of Padua, via Loredan 20, I-35131 Padova (Italy)*

Abstract

We present new theoretical and empirical results on the probability distributions of species persistence times in natural ecosystems. Persistence times, defined as the timespans occurring between species' colonization and local extinction in a given geographic region, are empirically estimated from local observations of species' presence/absence. A connected sampling problem is presented, generalized and solved analytically. Species persistence is shown to provide a direct connection with key spatial macroecological patterns like species-area and endemics-area relationships. Our empirical analysis pertains to two different ecosystems and taxa: a herbaceous plant community and a estuarine fish database. Despite the substantial differences in ecological interactions and spatial scales, we confirm earlier evidence on the general properties of the scaling of persistence times, including the predicted effects of the structure of the spatial interaction network. The framework tested here allows to investigate directly nature and extent of spatial effects in the context of ecosystem dynamics. The notable coherence between spatial and temporal macroecological patterns, theoretically derived and empirically verified, is suggested to underlie general features of the dynamic evolution of ecosystems.

Keywords: Biodiversity, Sampling Problems, Spatial Ecology, Macroecology, Neutral Ecological Theory

1. Introduction

Extinction rates, pointedly from habitat loss, have been defined as a crucial conservation problem of this century (Raup and Sepkoski, 1984; Wilcox and Murphy, 1985; Pimm et al., 1988; Fahrig, 1997; Ferraz et al., 2003). Direct and reliable estimation of true extinction rates remains problematic, however, and a lively debate exists over the possible overestimation of extinctions incurred through the standard use of methods based on the reversing of the species-area relationship (SAR), i.e. the number of species observed at increasing sampled areas (Green and Ostling, 2003; He and Hubbell, 2011).

Recently Bertuzzo et al. (2011) have proposed empirical and theoretical evidence for a new macroecological pattern, namely the distribution of persistence times for trophically equivalent, co-occurring species. The species persistence time (SPT) is defined as the time-span incurred between a species' emergence and its local extinction in a given geographic region. Using two different long-term ecological databases, related namely to the inventory of North American breeding birds and to Kansas grasslands, Bertuzzo et al. (2011) suggested that the empirical SPT distribution is characterized by a power-law function limited by an exponential cut-off determining the maximum observed persistence time, which in turn is related to the spatial extent of the ecosystem. The advantage to concentrate on SPTs, is that SPT distributions have proved to be a robust measure of species turnover at different spatial scale. Although SPT distributions cannot provide predictions about extinction rates of specific species, they can describe the global evolution of the diversity of an ecosystem and give robust estimates for mean SPTs (Bertuzzo et al., 2011).

The problem of the scale of observation becomes central in this framework. In fact, at the local scale, say an observational site for the presence/absence of breeding birds, the persistence time of a species is controlled by ecological processes operating at short timescales, like birth/death, dispersal, and contraction/expansion of geographic ranges. At this scale local extinctions are dynamically balanced by colonizations (MacArthur and Wilson, 1967; Tilman, 1994; Ricklefs and Scheuerlein, 2003; Muneepeerakul et al., 2008). At the global scale, species emergence and extinction are controlled by mechanisms acting on evolutionary timescales (Brown and Kodric-Brown, 1977; Diamond, 1989). Interestingly, the scaling behavior proposed by Bertuzzo et al. (2011) to govern the transition from local to global scales is capable of effectively describing the overall dynamical evolution of the ecosystem di-

versity. Scaling features also allow to predict SPT distributions for wide geographic areas from measures of persistence on smaller areas, which are much easier to monitor.

To provide a theoretical explanation for the SPT pattern, Bertuzzo et al. (2011) resorted to a spatially explicit model based on neutral theory. Neutral theory has been proposed as a unifying theoretical context for understanding ecological patterns (Hubbell, 2001). Since its formulation, several studies have focused their attention on it (e.g. Volkov et al., 2003; Houchmandzadeh and Vallade, 2003; Chave, 2004; Alonso and McKane, 2004; Azaele et al., 2006; Muneepeerakul et al., 2008; Chisholm and Lichstein, 2009). Neutral models are based on the assumption that, within a single trophic level, individual birth and death rates are species-independent. The main advantages of neutral models are that they are falsifiable, and that they are able to generate predictions for many different macroecological patterns. This is the case, for instance, of the relative species abundance (RSA) distribution (McGill, 2003; Volkov et al., 2005), the species-independent beta diversity patterns (Condit et al., 2002; Zillio et al., 2005), species geographic range (Bertuzzo et al., 2009) and the species-area relationship (Brown, 1995; Zillio et al., 2008; O'Dwyer and Green, 2010). Remarkably, this is accomplished by invoking only basic ecological processes such as birth, death, migration and dispersal limitation. Although certain emergent ecological patterns are independent of the fine ecological details and often well predicted by neutral theory (Bell, 2001), this does not imply that the underlying ecological processes are neutral (Harte, 2003; Purves and Pacala, 2005). Although the SPT distribution framework does not necessarily require neutral processes as well, we shall keep them as a reference modelling frame for our theoretical speculations.

This paper explores the subject of the SPT distribution further by extending the empirical and theoretical analysis presented in Bertuzzo et al. (2011). In particular, we report here on the study of two new long-term datasets to test the robustness of the SPT macroecological pattern. Moreover, we study in details the connections of the SPT distribution with the structure of the SAR and the endemics-area relationship (EAR, which gives the number of species that are confined within the sampled area; see Kinzig and Harte, 2000). We also investigate the role of spatial interactions in the new SPT data and show that the effect of the environmental matrix (Ricketts, 2001) on SPT distributions depends on the overall geographic area in which the ecosystem is embedded: if the typical dispersal range is compa-

rable to the total area, possibly because of dispersal limitation, then spatial interactions may be neglected. Finally we present and solve analytically a new particular case of a length-biased sampling problem (Cox, 1969) that arises in SPT data analysis; namely we find how to relate the SPTs derived from finite observational windows to the inherent SPT distribution of the ecosystem.

The paper is organized as follows: in the next section we briefly summarize the spatially explicit model for SPTs. In subsection 2.1 we discuss the effects of data sampling on SPT distributions. We present a general mathematical framework to relate SPT theoretical distributions to those obtained from finite samples. In the third Section, we present novel empirical SPT distributions regarding two different ecosystems (a forest in New Jersey and an assembly of estuarine fish in the Bristol Channel) and compare them with the distributions predicted by the neutral theory. The role of spatial scales and their interactions with SPT distributions, and the intimate relation between the SPT distribution and the SAR/EAR are also shown. A set of conclusions closes the article.

2. The Model

Neutral theory (Hubbell, 2001), which assumes that all the individuals within a given trophic level are competitively equivalent, offers a benchmark dynamics suggesting that many aspects of real biotic patterns may not require a more complex model (Muneepeerakul et al., 2008; Bertuzzo et al., 2009). According to the assumption of neutrality (Hubbell, 2001), the dynamics of a species in the ecosystem is fully specified by its effective birth and death rates $b(n)$ and $d(n)$, which depend exclusively on the population size n. Species abundance dynamics is described by the so called birth-death master equation (ME) (Volkov et al., 2003; Houchmandzadeh and Vallade, 2003):

$$\frac{dP(n,t)}{dt} = b(n-1)P(n-1,t)+d(n+1)P(n+1,t)-(b(n)+d(n))P(n,t), \quad (1)$$

where $P(n,t)$ is the probability, for a given species, of having a population of n individuals at time t. We note that $b(n)$ and $d(n)$ take into account several ecological processes that may increase or decrease the number of individuals in a species over time as, for instance, immigration or emigration. Assuming absorbing boundary conditions in $n = 0$, the probability density function

(pdf) of the theoretical persistence time p_τ can be expressed as (Pigolotti et al., 2005):

$$p_\tau(t) = \frac{dP(0,t)}{dt}. \tag{2}$$

Considering $b(n) = n(1-\nu)$ and $d(n) \propto n$, the above model describes analytically the mean field dynamics (in the limit of infinite number of nodes) of the following lattice model, known as the voter model (Holley, 1975; Durrett and Levin, 1996; Zillio et al., 2005). ν is termed diversification rate and it measures the frequency of appearance of new species in the system. Let us consider, for simplicity, a system with N nodes ($N \to \infty$). Each node may be occupied by a single individual belonging to a species which is represented by a given color. The dynamics at each time step is as follows. A randomly selected individual dies. With probability ν this site is occupied by a new species; with probability $1-\nu$, the site is colonized by an offspring of a node randomly chosen in the lattice (mean field case). We note that in this framework we require that the probability that a new species enters the system be uniformly distributed in time. This seems like a reasonable assumption in the absence of strong environmental or historical gradients within the considered timescale.

The spatial version of this model allows colonizations to occur only from one of the neighbors of the empty patch (i.e. dispersal limitation). The same model can be applied to 1D/3D lattices, or to a networked environment where dispersal is constrained directionally. By tracking every individual up to a statistically stationary state, it is possible to build the time series of species abundances and, from it, to compute numerically the SPT distribution. SPTs prove crucially dependent on the type of spatial connectivity interactions in the voter model. Exact and numerical results for the spatial voter model (Bertuzzo et al., 2011), in fact, show that the SPT distribution is consistent with power-law shapes of the type:

$$p_\tau(t) = \mathcal{C} t^{-\alpha} e^{-\nu t}, \tag{3}$$

where the scaling exponent α strictly depends on the connectivity structure and $\mathcal{C} = \nu^{1-\alpha}/\Gamma(1-\alpha)$ is the normalization constant ($\Gamma(x)$ is the complete Gamma function of argument x). The neutral model thus predicts the same functional shape for the STP distribution, a power law with the exponent α that is solely determined on the connectivity structure of the environment (Figure 1). Therefore α may be seen as a critical exponent (Stanley, 2000)

that is, it describes the behavior of physical systems near phase transitions. In general it is argued that scaling exponents do not depend on the details of the physical system, but only on the dimension D of the system (e.g. $D = 1$ on a line, $D = 2$ on an isotropic lattice and so on) or the range of the interactions (Stanley, 2000). This is not the first time that similarities between ecosystem dynamics and critical systems in physics have been pointed out (Banavar et al., 1999; Zillio et al., 2008).

From Monte Carlo simulations of the spatial voter model, α exponents for different geometric cases can be evaluated. It has been shown (Bertuzzo et al., 2011) that $\alpha \approx 1.5$ for the 1D lattice, $\alpha \approx 1.62$ for the networked landscape, $\alpha \approx 1.82$ and $\alpha \approx 1.92$ respectively for the 2D and 3D lattice (Figure 1). In the mean field case, the scaling limit ($\nu \ll 1$) of $p_\tau(t)$ can be calculated exactly (Pigolotti et al., 2005) yielding $p_\tau(t) \sim t^{-2} f(\nu t)$, with $f(z) = (z/(1-e^{-z}))^2 e^{-z}$. The robustness of the scaling behavior as a function only of the structure of the environmental matrix of interactions is deemed remarkable.

2.1. An Ecological Length-Biased Sampling Problem

Empirical data on persistence times for different species are available, especially from succession studies and long-term ecological databases (Pigolotti et al., 2005; Bertuzzo et al., 2011). However, for further empirical analysis, sampling effects on SPTs need to be taken into account. This type of sampling problem belongs to the class of so called length-biased problems, that arise in a wide range of different disciplines (Patil and Rao, 1978; Vardi, 1982).

We start with a thought experiment which we refer to as the stick-length sample problem. Consider an infinite number of sticks of different random length L distributed according to some unbiased pdf, say p_L. Imagine to place randomly these sticks on a plane x-y, aligned in the same direction (e.g. along the x direction). The process is thus defined in a 1D space, and the y axis is just a way to visualize different realizations of the same process. We denote by X^0 the position of the left side of a given stick. X^0 is a random variable uniformly distributed in $(0, \infty)$. Consider only those sticks that cross a vertical line $x = x^*$ and measure the lengths of those sticks (Figure 2).

We will denote by p_{L_c} the length distribution of this sticks sample. The stick-length sample problem can be formulated with the following questions: a) how is p_{L_c} related to p_L? b) How are the left and right ends of the sticks

that cross x^* (indicated by L_p, Figure 2) distributed? We now show how length measurements on particular samples of the stick population give length distributions which are different from that of the whole stick population.

Using tools of probability theory, it can be shown (Appendix A) that the pdf of the length of the sticks that cross x^*, in the limit $x^* \to \infty$ (to avoid boundary effects), is

$$p_{L_c}(l) = \frac{l p_L(l)}{\langle L \rangle}, \tag{4}$$

where $\langle L \rangle = \int_0^{+\infty} L p_L(L) dL$ is the average stick length. Thus the length pdf of the sample constituted by those sticks that cross the observation point x^*, p_{L_c}, is not the same as the overall population stick length pdf, i.e. p_L.

Let us now introduce a second vertical line $x = \hat{x} < x^*$. We now want to measure the length of the portions of sticks L_p crossed by the two vertical lines ($x = \hat{x}$ and $x = x^*$) that are comprised inside the space window $\Delta x = x^* - \hat{x}$ (see Figure 2). If we denote by p_{L_p} the pdf of L_p, then it can be shown (Appendix A) that:

$$p_{L_p}(l) = \frac{\int_l^{\infty} p_L(L) dL}{\langle L \rangle}. \tag{5}$$

Finally, we can calculate the pdf $p_{L'}$ of the random variable L' describing the length of a stick that is totally or partially comprised within the sampling window Δx. We note that in this case the maximum measured length of a stick is $\max\{L'\} = \Delta x$. L' can be expressed as a function of the other independent random variables L and X^0, that have already been probabilistically characterized. in fact, we can distinguish four different cases (see Figure 3):

- the stick is completely inside the window, then $L' = L$;
- $X^0 > \hat{x}$ and the stick crosses $x = x*$, then $L' = x^* - X^0 = L_p$
- $X^0 < \hat{x} < L + X^0 < x^*$ and the stick crosses $x = \hat{x}$, then $L' = X^0 + L - \hat{x} = L_p$;
- the stick is longer that the space window, then $L' = \Delta x$.

As explained in detail in Appendix A, we find that:

$$p_{L'}(l) \;=\; \frac{1}{\mathcal{N}}\Big((\Delta x - l) p_L(l) \Theta(\Delta x - l) \;+$$

$$
\begin{aligned}
&+ \quad \Theta(\Delta x - l) \int_{l>0}^{\infty} p_L(L) dL \; + \\
&+ \quad \Theta(\Delta x - l) \int_{l>0}^{\infty} p_L(L) dL \; + \\
&+ \quad \delta(l - \Delta x) \int_{\Delta x}^{\infty} (l - \Delta x) p_L(L) dL \Big), \qquad (6)
\end{aligned}
$$

where $\mathcal{N}$ is the normalization constant for $p_{L'}$, and $\delta(x)$ and $\Theta(x)$ are the Dirac delta distribution and the Heaviside step function, respectively. The last term of equation (6) gives an atom probability in $L = \Delta x$ corresponding to the fraction of sticks longer than the total length of the observational window ($\max\{L'\} = \Delta x$).

The probability distribution p_{L_I} of the sticks' length inside the window Δx follows directly from the first term of equation (6):

$$
p_{L_I}(l) \; = \; \frac{1}{\mathcal{N}'} (\Delta x - l) p_L(L) \Theta(\Delta x - l), \qquad (7)
$$

where $\mathcal{N}'$ is a proper normalization constant.

The analytical results provided by Eqs. (6) and (7) are tested via numerical simulation, as shown in the bottom panel of Figure 2. First we generate 10^5 segments along the $x-axis$ of random length drawn from an exponential pdf, i.e. $p_L(l) = \lambda e^{-\lambda l}$. Afterwards, we consider only those segments that are within the spatial window $\Delta x = 1/\lambda$ and we reconstruct the stick length pdf p_{L_I}. Analogously, we build $p_{L'}$. Finally we compare the numerical distributions with the the solution of Eqs. (6) and (7). As expected the agreement is perfect.

2.1.1. Application to SPTs.

Several real ecological sampling problems, both in time and space, can be mapped into the thought experiment described in the previous Section. In particular we now apply these results to SPTs.

Assume that species abundance (or presence-absence) time series for a given ecosystem characterized by a single trophic level are available from field campaigns carried on in a time period of span $\Delta t_w = t_f - t_0$ years. From the collected data, SPTs can be measured and the empirical SPT distribution likewise obtained. This distribution does not correspond to the theoretical SPT distribution, p_τ, in the same way as $p_L \neq p_{L'}$ in the stick

sample problem. In particular, $p_\tau(t)$ is affected by the fact that species persistence can be recorded only within a finite temporal window Δt_w. Thus, given the theoretical persistence-time pdf described by Eq. (3), we are interested in the pdfs of the variables that we can actually measure, i.e. the persistence times τ' of those species emerging before or during the observations and that are still present or go locally extinct within the time window Δt_w (and the persistence time τ_I of only those species that emerge and go locally extinct within the observed time window).

In our theoretical framework, the probability of a diversification event in a time step is constant. Thus the emergences of new species in the system obey a Poisson process, say $U(t)$, with rate $\lambda = \nu N$, where N is the total number of individuals in the system and λ has the dimensions of the inverse of (generation) time. Consequently the emergence times T^0 of species in the system are uniformly distributed. Therefore, we can map exactly this situation into the previous stick-length sample problem, with SPTs replacing stick lengths, i.e. $L \to \tau$, $L' \to \tau'$, $L_I \to \tau_I$ and $X^0 \to T^0$. Eqs. (6) and (7) allow us to test the theoretical SPT pdf $p_\tau(t)$ obtained by the spatial model against the empirical SPT distribution obtained from the measurements.

It is interesting to note how our thought experiment uses similar approaches to the model known as the mid-domain effect, which describes how species ranges that are randomly shuffled within a bounded geographical domain overlap increasingly toward the center of the domain, creating a mid-domain peak of species richness (Colwell et al., 2004; Arita, 2004). In fact, SPTs are essentially distributions of species temporal ranges, and therefore, the sampling problem just presented may be interpreted as a sort of mid-domain problem in time. However there is a crucial difference between the two effects: while for spatial ranges there are physical geometric constraints imposed by hard boundaries in space (i.e. geographic boundaries), and thus species spatial ranges must be contained within the given geographic region (Colwell et al., 2004; Arita, 2004), temporal ranges do not have constraints in time. It is in fact to be reminded that species temporal ranges are not limited by the observational time window, rather is our capacity to measure real species temporal ranges that is limited.

3. Results.

3.1. Empirical SPTs and Comparison with Model Results.

Bertuzzo et al. (2011) presented a comparison between the theoretical

model and the empirical SPT distributions for two different ecosystems (North American breeding birds and Kansas grassland) which is shown in Figure 4a,b for purpose of completeness.

We now provide new evidence of the existence and robustness of the SPT distribution pattern by presenting empirical data on persistence times taken from two different ecological databases and comparing them with the analytical results on SPT distributions. Specifically, we empirically characterize SPT distributions of two long-term datasets concerning ecosystems with very different characteristics: 1) a 44-year long study from the Buell-Small Succession (BSS) Study of plants in New Jersey ; and 2) a 28-year long database of British estuarine fish collected at Hinkley Point (headland on the Bristol Channel coast of Somerset, England).

The BSS study (Institute of Ecosystem Studies, 2008) includes ten fields that were released from agriculture and used to study succession dynamics. Permanent plots, measuring 48 m^2 each, were established in every field. The permanent plots were sampled every year from 1958 to 1979, after which they were sampled alternatively every other year to the present day. The fields differ in the year of release, thus we consider only data collected after the latest field abandonment year (1968). In order to avoid missing data in alternate years, the minimum sampled area (afterwards named cell) considered in the calculation of the empirical SPT distributions comprises two adjacent fields (96 m^2). In this way each cell is populated with presence-absence records for each year. We repeat the same analysis for 3 other different scales: 4,6,8 adjacent fields (A=192, 288, 384 m^2, respectively). We also analyze the whole system, which corresponds to an area of $A = A^* = 480$ m^2. For every scale A of analysis, the presented results refer to the average over all possible combinations of adjacent plots within the system (moving average procedure). A three-dimensional presence-absence matrix P is in this way built. Each element P_{stc} of the matrix is equal to 1 if species s is observed during year t in a cell c, otherwise $P_{stc} = 0$. The empirical SPT is defined as the number of consecutive years in which the measurements reveal the presence of the species in that geographic region (see Figure 3). For every cell c and every species s we measure persistence times from presence-absence time series derived from the second dimension/index of matrix P. The presence-absence time series thus form a vector of length T, where T is the total number of years of observation, that has as j-th component a one if species s is observed in cell c during the j-th year. Persistence time is defined as the length of a contiguous sequence of ones in the time series (Figure 3). For every scale

of analysis we consider all the measured persistence times regardless of the species they belong to, and we build the SPT empirical pdf at every cell scale (Figure 4c).

As for the second database, fish samples were collected from the cooling-water filter screens at Hinkley Point B Power Station, situated on the southern bank of the Bristol Channel in Somerset (England) from 1980 to 2008. A full description of the intake configuration and sampling methodology is given in Magurran and Henderson (2003). We only consider estuarine fish species (not crustaceous organisms). Empirical SPT pdf's can be computed as described for the BSS dataset (Figure 4d). Note, however, that in this dataset there is no spatial scale variability, because the samples were collected in a single point in space. Therefore we limit our analysis to a single spatial scale.

Using Eqs. (6) and (7) and the observational data we performed the best fit of α and ν, the parameters of the theoretical SPT pdf. At any spatial scale, the scaling exponent and the diversification rate for the empirical SPT distributions are determined with a simultaneous nonlinear fit of observational and analytical pdfs of τ' and τ_I. Table 1 summarizes the results of the fit. Remarkably, in both cases the scaling exponents derived empirically are consistent with those predicted by the neutral voter model. In particular, for the fishes we find $\alpha = 1.97 \pm 0.06$, which is compatible with the exponent $\alpha = 2$ predicted by the mean field voter model (see Figure 4d). In fact, no spatial information is embedded in our empirical data and thus we do not expect to see the effect of dispersal limitation on the relevant ecosystem dynamics. Figure 4c shows the case of the New Jersey plant communities, for which the best fit of p_τ is $\bar{\alpha} = 1.97 \pm 0.12$ (where $\bar{\alpha}$ is the average of the exponents over all the cell scales), which is also compatible with the mean field prediction $\alpha = 2$. In this case the negligible effects of dispersal limitation on the ecosystem dynamic suggests that the average plant dispersal radius R is comparable with the linear dimension of the total sampled area, i.e. $R \approx \sqrt{A^*}$, and thus the net result is a mean field dynamics not affected by spatial interactions (Bertuzzo et al., 2011). The fact that the total sampled area of the ecosystem is very small ($A^* = 480$ m^2) strongly supports this interpretation of the data.

While studying SPTs in a given ecosystem on the basis of presence/absence (or count) data, imperfect detection of species is a source of concern (Nichols et al., 1998). Species, in particular animal species, are, in fact, routinely sampled with a detection probability much smaller than one. Although in general

the problem of imperfect detection is somewhat less relevant for herbaceous plant datasets, in the case of the BSS forest sampling occurs either annually or biannually, e.g. implying that seasonal variability in plant composition may be not picked up (and this varies from year to year). However, plants that go undetected because of yearly sampling affect the estimates of persistence times shorter than one year, thus not an issue for the scaling of SPTs. Moreover, plants in vegetative state are not identifiable, nor are small recruits, typically. For the fish database the power station intakes at Hinkley Point are an effective sampler because of their location at the edge of a large inter-tidal mudflat in an estuary. The filter screens have a solid square mesh of 10 mm and start to retain fish of standard length of about 25 mm (Henderson and Holmes, 2001). A 99% retention for many species occurs at the standard length of 40 mm. Nevertheless, incomplete sampling is present because only a small fraction of the water in the Bristol channel is filtered, and filtering thus only catches fish that cannot avoid being sucked by the water turbines. Hence, even in intensive sampling programs is difficult to tell whether absences are real or caused by incomplete detection/sampling. Note that the impact of imperfect sampling on SPTs of North America breeding birds has been analyzed in details in (Bertuzzo et al., 2011). However, we acknowledge that to show that SPTs are generally a more robust alternative to estimating extinction rates, a systematic and widespread analysis of the effect of incomplete sampling and detection on SPTs needs to be undertaken. This is still lacking and will be tackled in details in future works.

3.2. Relations among SPT, SAR and EAR

The SPT distribution is also particularly interesting because it generates spatial patterns that can be related, within our theoretical framework, to other important macroecological patterns, as the SAR and the EAR relationships. We can use the BSS data at different spatial scales to investigate how SPTs can give information also on the biogeography of the BSS plant ecosystem. In fact, the scale-invariant character of p_τ indicates that α depends only on the spatial connectivity of the environment (i.e. networked, $2D, ..$), and not on the sampling area. On the contrary ν, which accounts for immigration processes from species outside the local community, is argued to decrease with increasing sampling area, thus representing a clear signature of the geographic scale of the analysis. The SAR characterizes how the average number of observed species increases with increasing sample area and it is usually characterized by a power-law behavior, i.e. $S \sim A^z$ (Brown, 1995).

Our theoretical framework allows for the linkage of the cut-off timescale $1/\nu$ with the spatial scale of analysis, and the SPT distribution to the SAR. In fact, in the neutral model, species emerge as a point Poisson process with rate νN and last for a lifetime τ . Therefore, the mean number of species in the system at stationarity is $\langle S \rangle = \nu N \langle \tau \rangle$ (Bertuzzo et al., 2011). By deriving the scaling behavior of ν, N and $\langle \tau \rangle$ with respect to A, we can thus make a connection between SPTs and the SAR.

The last term in Eq. (6) represents the analytical expression of the fraction of species that are present during the whole observational time period ($\mathcal{S}(\Delta t_w)$). It provides a tool to quantitatively estimate the diversification rate from the empirical SPT pdf. In fact, in order to infer with better precision ν from the observational data, we numerically find the value of ν that minimizes $\mathcal{S}(\Delta t_w)$ at every different spatial scales A (see Appendix C for details) using the scaling exponent $\bar{\alpha}$. The best fit of the scaling law between ν and A obtained in this way gives $\nu \sim A^{-\beta}$, with $\beta = 1 \pm 0.1$ (Figure 5a), thus confirming that the diversification time ν^{-1} scales almost linearly with the area (Zillio et al., 2005).

Once the scaling law between ν and A is established, in order to derive the SAR, we need to estimate the scaling between the total number of individuals N and the sampled area A. In Bertuzzo et al. (2011) an isometric relation $N \propto A$ (MacArthur and Wilson, 1967) was assumed. However the abundance data on the New Jersey plant communities show that this is not the case for that ecosystem. In fact the average total species coverage percentage over all the plots is 165%. Samplers start with the topmost layer, usually the trees, and work their way down to the species closest to the ground (Institute of Ecosystem Studies, 2008). Thus the exceedance in the coverage percentage is due to the overhanging among species. In order to evaluate the scaling relation between N and A, we then build a minimalist model, in which species are classified by their typical average size. Assuming biotic saturation, i.e. that each species covers completely the sampling region, in a plot of area A we can find at most $[A/a]$ individuals of characteristic size area $a \ll A$ ($[x]$ denotes the smallest integer not greater that x), $[A/2a]$ individuals of characteristic area $2a$ and so forth. In general, the total number of individuals N in a region of area A scales as

$$N(A) \propto \sum_{n=1}^{[A/a]} \frac{A}{na} \sim \frac{A}{a} H_{A/a}, \tag{8}$$

where $H_q = \sum_{n=1}^{q} 1/n$ is the harmonic number and $H_{A/a} \sim \ln(A/a)$. The constant of proportionality in Eq. (8) depends on the arbitrary choice of a. However since $H_{A/a} \sim \ln(A/a)+$ sub-leading terms, a change of a in λa leads to $H_{\lambda a} = \frac{1}{\lambda} H_{A/a}+$ sub-leading terms and so its precise value is irrelevant since it can be absorbed in the proportionality constant (see below) to be determined from the best fit of the data.

Finally, we calculate the asymptotic behavior of the mean SPT $\langle \tau \rangle = \int t p_\tau(t) dt$ (see Appendix C for mathematical details) and we get:

$$\langle \tau \rangle \sim \begin{cases} A^{-\beta(\alpha-2)} & \text{for } \alpha < 2; \\ \ln(A) & \text{for } \alpha = 2. \end{cases} \tag{9}$$

Putting all the above scaling results together, we find that for the BSS plant ecosystem (which is characterized by $\alpha \approx 2$) the mean-field neutral framework predicts a power-law SAR with logarithmic correction:

$$\langle S(A) \rangle = K A^{1-\beta} \ln(A)\, H_A, \tag{10}$$

where K is the constant of proportionality. We determine the constant K in three different ways: 1) through the best fit of Eq. (10) on the empirical SAR data; 2) by imposing that in the total area A^* we have the total number of species S^*; 3) by finding the value of K that gives the exact number of species in the smallest area ($A = 96$ m^2) and then predicting the complete SAR curve (upscaling). Remarkably, all three methods yield $K \approx 3.46$. We also performed the best fit of the power-law SAR ($S \sim A^z$) on the empirical data, obtaining $z = 0.34$. We note that in our range of areas, this result it is not distinguishable from the SAR given by Eq. (10) as shown by Figure 5c.

In the special case of mean field interactions, we can also calculate the EAR. EAR is defined as the relation between the number of species endemic to a region and the area of that region (Kinzig and Harte, 2000; Green and Ostling, 2003). The EAR has been recently proposed by He and Hubbell (2011) as the correct approach in order to estimate extinction rates from habitat loss. The fact that the mean-field approach well describes the empirical SPT distribution suggests that in the BSS ecosystem the phenomenon of spatial aggregation or clustering is negligible. In fact mean-field dynamics indicates that species composition is well mixed in the ecosystem and thus it does not depend on spatial features. Therefore, in this case, we can evaluate the EAR curve just by reversing the SAR (He and Hubbell, 2011):

$$\langle E(A) \rangle = S^* - \langle S(A^* - A) \rangle = S^* - \ln(A^* - A)\, H_{A^*-A}, \tag{11}$$

where E is the number of endemic species. Figure 5 summarizes all the above results and shows the comparison between the empirical and theoretical results for the SAR and the EAR.

4. Conclusions

We have presented new theoretical and empirical evidence supporting the broad validity of a recently proposed macroecological pattern, the SPTs distribution. Specifically, we have completed (and described in detail) the theoretical treatment of the relevant ecosystem dynamics and of the derived sampling problem, and analyzed empirically two further rather diverse ecosystems (hosting respectively herbaceous plants and estuarine fishes). In both cases the observed SPT distributions display a power-law shape with a cut-off due to the finiteness of the observational time window, which is reproduced by the theoretical model. These results are expected to be robust with respect to relaxations of specific assumptions on ecological neutrality (Bertuzzo et al., 2011), thus confirming our expectation that power laws, observed for SPT pdfs, are the result of emergent behaviors independent of fine details of the system dynamics.

The specific values of the scaling exponents of the SPT distributions depend only on a few key factors, namely the spatial dimension of the embedding ecosystem matrix and the nature of dispersal limitation. In particular, our results show that dispersal limitation does not occur in the ecological dynamics of both ecosystems under study. While this result could be expected for the estuarine fishr inventory, where data were collected at a single point in space, quite surprisingly the BSS plant community does not show signs of dispersal-limited spatial interactions. We interpret this result as a consequence of the fact that the total sampled area in the BSS forest is very small. This suggests that the average plant dispersal radius is comparable to the characteristic size of the ecosystem, thus complying to mean-field-like dynamics.

Because of the assessed, robust scale invariance character of the SPT distribution (limited only by biogeographical finite-size effects), and because of its relation with other macro-ecological patterns, we have proposed that the SPTs distribution is a powerful synthetic descriptor of ecosystem biodiversity and of its associated dynamics.

New data would allow for the investigation of other implications of the theoretical predictions. For instance, the neutral voter model predicts that

the scaling exponents of the SPT distributions of riparian ecosystems (i.e. networked environments where directional, anisotropic dispersal is forced by the structure of the fluvial environmental matrix) should be lower than those of 2D, 3D or mean-field ones. This result, if proven, would have remarkable consequences for conservation ecology, because it suggests that species that disperse isotropically have shorter average persistence times than species that are constrained to disperse along spatially constrained and anisotropic ecological corridors, like those provided by river networks. This, in turn, calls for long-term analysis of riparian ecosystems to test empirically the effects of river morphology on ecosystem dynamics.

For these reasons we suggest that field biologists and ecologists should perhaps invest renewed efforts in collecting improved long-term datasets of ecosystem dynamics at different spatial and temporal scales and under different dispersal conditions (for instance, archives beyond presence/absence of species within networked environments like riverine ecosystems for freshwater fish) as they prove crucial for our deeper understanding of universal patterns in macroecology. The present study shows that long-term datasets can be profitably used to highlight crucial properties and spatial effects of ecosystem dynamics, including the role played by the underlying connectivity structure in shaping SPT distributions.

Acknowledgments
We are grateful to Pisces Conservation Conservation and to Dr. P. Henderson for granting us open access to the Hinkley fish database. We acknowledge the BSS research group for making their data available through the NSF grant DEB 97-26992 (Long-Term Research in Environmental Biology). We acknowledge two reviewers for their suggestions and comments that have been instrumental in our revision, and have remarkably improved the manuscript. SS, EB, LM and AR gratefully acknowledge the support provided by ERC advanced grant program through the project RINEC-227612 and by the SFN/FNS project 200021_124930/1. IRI gratefully acknowledges the support of the James S. McDonnell Foundation through a grant for Studying Complex Systems (220020138). AM acknowledges funds provided by Fondazione Cariparo (Padova, IT).

Appendix A.

In this appendix we derive the analytical results of the stick-length sample problem presented in the main text. The set up of the thought experiment is fully described in the main text and in Figure 2.
Specifically, the stick-length sample problem can be characterized by five random variables, namely: i) X^0 is the position of the left side of a given stick; ii) L describes the length of a stick; iii) L_c is the length of those sticks that cross x^*; iv) L_p is the length of that part of the stick that crosses x^* or $\hat{x}$ and fall within Δx; v) L' is the length of a stick that is totally or partially comprised inside Δx.
X^0 and L are the two independent random variables of the problem, while L_c, L_p and L' can all be expressed in terms of X^0 and L, as we will show in details. Assuming that p_L is the unbiased length stick distribution, we now present a methodology that enable us to derive the length pdf p_{L_c}, and the pdf p_{L_p} as a function of p_L. The same methodology may be applied to obtain $p_{L'}$
The random variable L_p can be expressed as a function of the random variables L and X^0. In fact, we have that the sticks that cross x^* are those for which $X^0 < x^*$ and $X^0 + L > x^*$ (see Figure 2). Therefore, if Θ is the Heaviside step function, the length of a stick that crosses x^* is given by the random variable

$$L_c = L\Theta(X^0 + L - x^*)\Theta(x^* - X^0). \tag{A.1}$$

We know that L is distributed ($\sim$) as p_L and that X^0 is uniformly distributed along the x-axis (in particular $X^0 \sim U_{(0,x^*)}$). Therefore we have that the probability density function (pdf) p_{L_c} is

$$p_{L_c}(l) = \frac{\langle \delta(l - L)\Theta(X^0 + L - x^*)\Theta(x^* - X^0)\rangle}{\langle \Theta(X^0 + L - x^*)\Theta(x^* - X^0)\rangle}, \tag{A.2}$$

where δ is the Dirac delta function. The numerator of Eq. (A.2) simply gives the ensemble average, taken over the random variables X^0 and L, of different realizations of the event that occurs when a stick of length L intersects x^*, while the denominator in (A.2) assures the normalization condition.
In order to solve the ensemble average of the latter equation, we split the calculation into two steps. First we calculate the conditional probability

function $p_{L_c}(l|L)$ of a stick crossing the vertical line x^*, given the fact that it has a length L, i.e. we perform only the average over X^0

$$p_{L_c}(l|L) = \frac{\int_{\max[0,x^*-L]}^{x^*} \delta(l-L)dX^0}{\langle \Theta(X^0+L-x^*)\Theta(x^*-X^0)\rangle}. \tag{A.3}$$

As a second step, we marginalize Eq. (A.3) over L, i.e. we perform the average also over L:

$$p_{L_c}(l) = \frac{\int_0^{+\infty} p_L(L)\delta(l-L)\min[x^*,L]dL}{\int_0^{+\infty}\min[x^*,L]p_L(L)dL}. \tag{A.4}$$

Assuming that we do not have boundary effects (i.e. $x^* \to +\infty$) we obtain Eq. (4) in the main text.
The case of L_p can again be obtained using the same technique. Writing the random variable L_p as a function of L and X^0 (see figure 2) we get

$$L_p = (x^*-X^0)\Theta(x^*-X^0)\Theta(X^0+L-x^*)\Theta(X^0). \tag{A.5}$$

Following the same steps presented before, we obtain

$$p_{L_p}(l|L) = \frac{\int_0^{\infty}\delta(l-(x^*-X^0))\Theta(x^*-X^0)\Theta(X^0+L-x^*)\Theta(X^0)}{\langle\Theta(x^*-X^0)\Theta(X^0+L_p-x^*)\rangle}, \tag{A.6}$$

and marginalizing over L we obtain

$$p_{L_p}(l) = \Theta(x^*-l)\frac{\int_0^{\infty}\Theta(L-l)p_L(L)}{\int_0^{+\infty}\min[x^*,L]p_L(L)dL}, \tag{A.7}$$

that, in the limit $x^* \to \infty$, results in Eq. (5). The case of a stick crossing $x = \hat{x}$ is perfectly symmetric to the one discussed above and would lead to the same result.
The results for L' and L_I follow similarly.

Appendix B.

In this section we present the calculations used to estimate the diversification rate ν from the empirical SPT distributions of the BSS plant community. We denote by $\mathcal{E}(\Delta t_w)$ the fraction of species, evaluated from the data, that are present during the whole observational time period Δt_w.

The last term in Eq. (6), denoted here as $\mathcal{A}_{\Delta t_w}$, gives the theoretical value of the latter quantity, i.e. the atom probability of the SPT distribution for $t = \Delta t_w$. By using the theoretical SPT distribution described by Eq. (3) we can estimate $\mathcal{A}(\Delta t_w)$:

$$\begin{aligned} \mathcal{A}_{\Delta t_w}(\nu) &= \int_{\Delta t_w}^{\infty} (\tau - \Delta t_w) \frac{\nu^{1-\alpha}}{\Gamma(1-\alpha, \nu t_{min})} \tau^{-\alpha} e^{-\nu\tau} d\tau \\ &= \frac{\Gamma(2-\alpha, \nu\Delta t_w) - \nu\Delta t_w \Gamma(1-\alpha, \nu\Delta t_w)}{\nu\Gamma(1-\alpha, \nu t_{min})}, \end{aligned} \tag{B.1}$$

where $\Gamma[a, b]$ is the incomplete Gamma function, and t_{min} is the minimum SPT observed in the ecosystem (in general $t_{min} \to 0$). If $\alpha < 2$, then the dependence of Eq. (B.1) on νt_{min} is weak, and thus, as $\nu t_{min} \ll 1$, we can set $\nu t_{min} \approx 0$.
Therefore we calculate the values of the diversification rate ν for a given Δt_w (that in turn depends on the specific sample area A) by numerically minimizing the quantity

$$\mathcal{S}(\nu|\Delta t_w) = (\mathcal{A}_{\Delta t_w}(\nu) - \mathcal{E}(\Delta t_w))^2, \tag{B.2}$$

where the average scaling exponent $\bar{\alpha}$ obtained by the best fit of the SPT pdf $p_{\tau'}$ and p_{τ_I} has been used for α . Eventually, repeating the same procedure using different time windows (corresponding to the different sampled areas) we obtain the scaling relation between ν and A presented in the main text.

Appendix C.

In this appendix we derive the asymptotic behavior of the mean persistence times $\langle\tau\rangle$. We divide the calculation into two cases: $\alpha < 2$, where the dispersal limitation is an important driver of the ecosystem dynamics and $\alpha = 2$, the mean field case. The mean persistence time for $\alpha < 2$ is

$$\langle\tau\rangle = \frac{\int_{\nu t_{min}}^{\infty} t^{1-\alpha} e^{-t} dt}{\nu \int_{\nu t_{min}}^{\infty} t^{-\alpha} e^{-t} dt} = \frac{\Gamma(2-\alpha, \nu t_{min})}{\nu\Gamma(1-\alpha, \nu t_{min})}. \tag{C.1}$$

Integrating by parts, the denominator of Eq. (C.1) becomes:

$$\Gamma(1-\alpha, \nu t_{min}) = \frac{(\nu t_{min})^{1-\alpha}}{\alpha - 1} + \frac{1}{1-\alpha}\Gamma(2-\alpha, \nu t_{min}), \tag{C.2}$$

and using the limit $\lim_{\nu t_{min}\to 0}\Gamma(2-\alpha,\nu t_{min})=\Gamma(2-\alpha)>0$, Eq. (C.1) simplifies to

$$\langle\tau\rangle\sim\nu^{\alpha-2}. \tag{C.3}$$

In the case $\alpha=2$ we have instead

$$\langle\tau\rangle=\frac{t_{min}E_1(t_{min}\nu))}{E_2(t_{min}\nu)}, \tag{C.4}$$

where $E_n(z)=\int_1^\infty e^{-zt}t^{-n}dt$ is the exponential integral function. The expansion of the exponential integral function for $x\approx 0$ is (Abramowitz and Stegun, 1965, pag. 229):

$$E_1(x) \sim -\frac{x^2}{4}+x-\log(x)-\gamma \tag{C.5}$$

$$E_2(x) \sim -\frac{x^2}{2}+x(\log(x)+\gamma-1)+1, \tag{C.6}$$

where γ is the Euler constant. Substituting the latter expansion into Eq. (C.4) we obtain

$$\langle\tau\rangle\sim -t_{min}(\log(\nu)+\gamma)\sim-\log(\nu). \tag{C.7}$$

Therefore we find that $\langle\tau\rangle$ scales as the logarithm of ν and, in turn, as the logarithm of the sampled area A (in fact we found that $\nu\sim A^{-1}$). The logarithmic correction in the scaling behavior of $\langle\tau\rangle$ is supported by the data (see Figure 5 in the main text) confirming the hypothesis that the evolution of the BSS ecosystem is well mimicked by mean field dynamics.

References

Abramowitz, M., Stegun, I., 1965. Handbook of Mathematical Functions. New York Press, Dover.

Alonso, D., McKane, J., 2004. Sampling Hubbell's neutral theory of biodiversity. Ecology 7, 901.

Arita, H., JAN 7 2004. Range size in mid-domain models of species diversity. Journal of Theoretical Biology 232 (1), 119–126.

Azaele, S., Pigolotti, S., Banavar, J. R., Maritan, A., 2006. Dynamical evolution of ecosystems. Nature 444 (7121), 926–928.
URL `http://dx.doi.org/10.1038/nature05320`

Banavar, J., Green, J., Harte, J., Maritan, A., 1999. Finite Size Scaling in Ecology. Physical Review Letters 20 (83), 4212–4214.

Bell, G., SEP 28 2001. Neutral macroecology. Science 293 (5539), 2413–2418.

Bertuzzo, E., Muneepeerakul, R., Lynch, H. J., Fagan, W. F., Rodriguez-Iturbe, I., Rinaldo, A., NOV 18 2009. On the geographic range of freshwater fish in river basins. Water Resour. Res. 45.

Bertuzzo, E., Suweis, S., Mari, L., Maritan, A., Rodriguez-Iturbe, I., Rinaldo, A., MAR 15 2011. Spatial effects on species persistence and implications for biodiversity. Proceeding of the National Academy of Science, USA 108 (11), 4346–4351.

Brown, J., Kodric-Brown, A., 1977. Turnover rates in insular biogeography – Effect of immigration on extinction. Ecology 58 (2), 445–449.

Brown, J. H., 1995. Macroecology. The University of Chicago Press, Chicago.

Chave, J., MAR 2004. Neutral theory and community ecology. Ecology Letters 7 (3), 241–253.

Chisholm, R. A., Lichstein, J. W., DEC 2009. Linking dispersal, immigration and scale in the neutral theory of biodiversity. Ecology Letters 12 (12), 1385–1393.

Colwell, R., Rahbek, C., Gotelli, N., MAR 2004. The mid-domain effect and species richness patterns: What have we learned so far? American Naturalist 163 (3), E1–E23.

Condit, R., Pitman, N., Leigh, E., Chave, J., Terborgh, J., Foster, R., Nunez, P., Aguilar, S., Valencia, R., Villa, G., Muller-Landau, H., Losos, E., Hubbell, S., JAN 25 2002. Beta-diversity in tropical forest trees. Science 295 (5555), 666–669.

Cox, D., 1969. Some sampling problems in technology. In: Johnson, U., Smith, H. (Eds.), In New Developments in Survey Sampling. Wiley, New York, pp. 506–527.

Diamond, J., NOV 6 1989. The present, past and future of human-caused exctinctions. Phil. Trans. Roy. Soc. B 325 (1228), 469–477.

Durrett, R., Levin, S., MAR 21 1996. Spatial models for species-area curves. Journal of Theoretical Biology 179 (2), 119–127.

Fahrig, L., JUL 1997. Relative effects of habitat loss and fragmentation on population extinction. Journal of Wildlife Management 61 (3), 603–610.

Ferraz, G., Russell, G., Stouffer, P., Bierregaard, R., Pimm, S., Lovejoy, T., NOV 25 2003. Rates of species loss from Amazonian forest fragments. Proceedings of the National Academy of Sciences of the United States of America 100 (24), 14069–14073.

Green, J., Ostling, A., NOV 2003. Endemics-area relationships: The influence of species dominance and spatial aggregation. Ecology 84 (11), 3090–3097.

Harte, J., 2003. Tail of death and resurrection. Nature 424, 1007.

He, F., Hubbell, S. P., MAY 19 2011. Species-area relationships always overestimate extinction rates from habitat loss. Nature 473 (7347), 368–371.

Henderson, P. A., Holmes, R., 2001. On the population dynamics f dab, sole and flounder within bridgwater bay in the lower severn estuary, england. Netherlands Journal of Sea Research 27 (3/4), 337–344.

Holley, R. snd Liggett, T., 1975. Ergodic theorems for weakly interacting infinite systems and voter model. Annals of Probability 3 (4), 643–663.

Houchmandzadeh, B., Vallade, M., DEC 2003. Clustering in neutral ecology. Phys. Rev. E 68 (6, Part 1).

Hubbell, S., 2001. The Unified Theory of Biodiversity and Biogeography. Princeton University Press.

Institute of Ecosystem Studies, 2008. Buell-Small succession study.

Kinzig, A., Harte, J., DEC 2000. Implications of endemics-area relationships for estimates of species extinctions. Ecology 81 (12), 3305–3311.

MacArthur, R., Wilson, E., 1967. The Theory of Island Biogeography. Princeton Univeristy Press.

Magurran, A., Henderson, P., 2003. Explaining the excess of rare species in natural species abundance distributions. Nature 422 (17).

McGill, B., APR 24 2003. A test of the unified neutral theory of biodiversity. Nature 422 (6934), 881–885.

Muneepeerakul, R., Bertuzzo, E., Lynch, H. J., Fagan, W. F., Rinaldo, A., Rodriguez-Iturbe, I., MAY 8 2008. Neutral metacommunity models predict fish diversity patterns in Mississippi-Missouri basin. Nature 453 (7192), 220–U9.

Nichols, J., Boulinier, T., Hines, J., Pollock, K., Sauer, J., 1998. Estimating rates of local species extinction, colonization, and turnover in animal communities. Ecol. Appl. 8 (4), 1213–1225.

O'Dwyer, J. P., Green, J. L., JAN 2010. Field theory for biogeography: a spatially explicit model for predicting patterns of biodiversity. Ecology Letters 13 (1), 87–95.

Patil, G. P., Rao, C. R., 1978. Weighted distributions and size-biased sampling with applications to wildlife populations and human families. Biometrics 34 (2), 179–189.

Pigolotti, S., Flammini, A., Marsili, M., Maritan, A., 2005. Species lifetime distribution for simple models of ecologies. Proceeding of the National Academy of Science, USA 102, 15747.

Pimm, S., Jones, H., Diamond, J., DEC 1988. On the risk of extinction. American Naturalist 132 (6), 757–785.

Purves, D. W., Pacala, S. W., 2005. Biotic Interactions in the Tropics. Cambridge Univ. Press.

Raup, D., Sepkoski, J., 1984. Periodicity of Extinctions in the Geologic Past. Proceedings of the National Academy of Sciences of the United States of America-Biological Sciences 81 (3), 801–805.

Ricketts, T., JUL 2001. The matrix matters: Effective isolation in fragmented landscapes. American Naturalist 158 (1), 87–99.

Ricklefs, R. E., Scheuerlein, A., 2003. Life span in the light of avian life histories. Pop. Develop. Rev. 29 (Suppl. S), 71–98.

Stanley, H. E., 2000. Scale Invariance and Universality: organizing principles in complex system. Physica A 281, 60–68.

Tilman, D., JAN 1994. Competition and biodiversity in spatially structured habitats. Ecology 75 (1), 2–16.

Vardi, Y., 1982. Nonparametric estimation in the presence of length bias. Annals of Statistics 10 (2), 616–620.

Volkov, I., Banavar, J., Hubbell, S., Maritan, A., AUG 28 2003. Neutral theory and relative species abundance in ecology. Nature 424 (6952), 1035–1037.

Volkov, I., Banavar, J. R., He, F., Hubbell, S. P., Maritan, A., 2005. Density dependence explains tree species abundance and diversity in tropical forests. Nature 438 (7068), 658–661.
URL http://dx.doi.org/10.1038/nature04030

Wilcox, B., Murphy, D., 1985. Conservation strategy - the effects of fragmentation on extinction. American Naturalist 125 (6), 879–887.

Zillio, T., Banavar, J. R., Green, J. L., Harte, J., Maritan, A., DEC 2 2008. Incipient criticality in ecological communities. Proceeding of the National Acadamy of Science, USA 105 (48), 18714–18717.

Zillio, T., Volkov, I., Banavar, J., Hubbell, S., Maritan, A., AUG 26 2005. Spatial scaling in model plant communities. Phys. Rev. Lett. 95 (9).

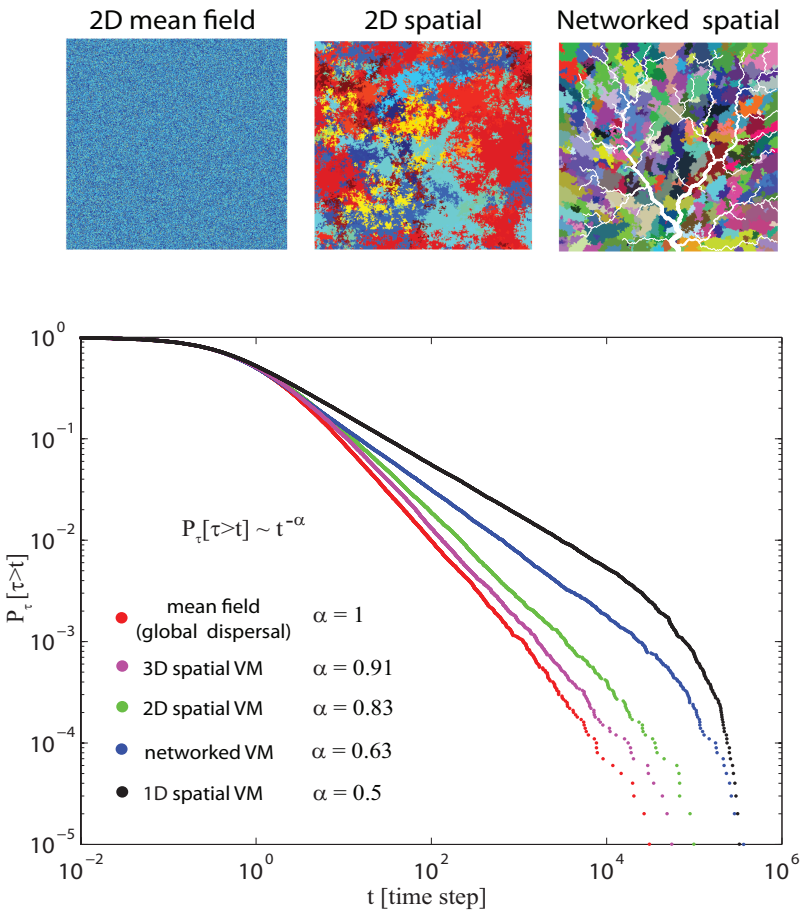

Figure C.1: (a) Persistence-time exceedance probabilities $P_\tau(t)$ (probability that species' persistence times τ be $\geq t$) for the neutral individual-based model with nearest-neighbor dispersal implemented on the different topologies (redrawn from Bertuzzo et al. (2011)). Species persistence time distributions are crucially dependent on the type of spatial connectivity interactions in the voter model.

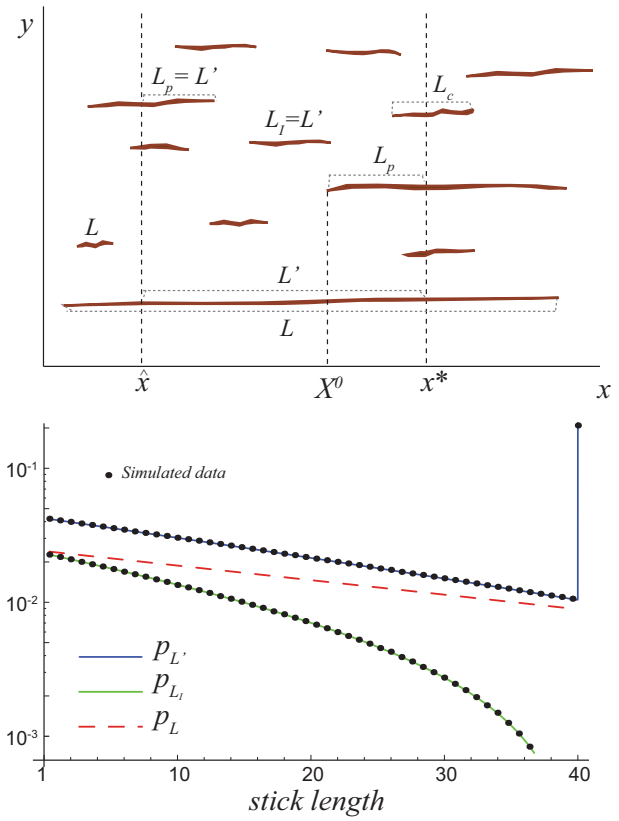

Figure C.2: Top panel: schematic representation of the stick-length sample problem. The variables that can be measured from the sample of sticks in Δx are L' and L_I, both with a different distribution with respect to $p(L)$. Bottom panel: comparison between analytical SPT pdfs $p_{L'}$ and p_{L_I} given by Eqs (6)-(7), and those obtained through numerical simulation of the stick length problem starting from an unbiased stick length distribution $p_L(l) = \lambda e^{-\lambda l}$, with $\Delta x = 1/\lambda$ (in this particular example $\lambda = 0.025$). p_L, p_{L_I} and $p_{L'}$ have been shifted in the semi-log y plot for clarity.

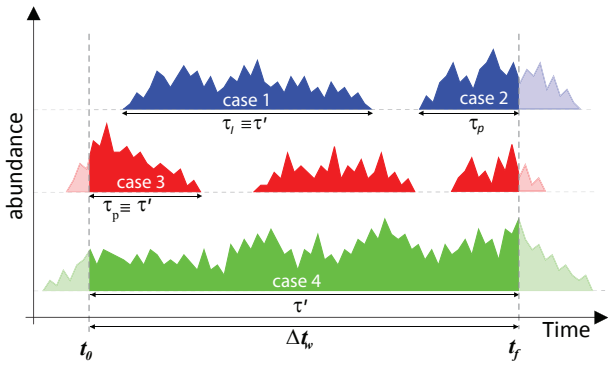

Figure C.3: The species persistence-time (SPT) within a geographic region is defined as the time incurred between a species' emergence and its local extinction. Recurrent colonizations of a species define different SPTs times. The SPTs τ_p, τ_I and τ', that can be measured within the observational window, are in general different from the unbiased SPT τ. The four different cases are discussed in the main text.

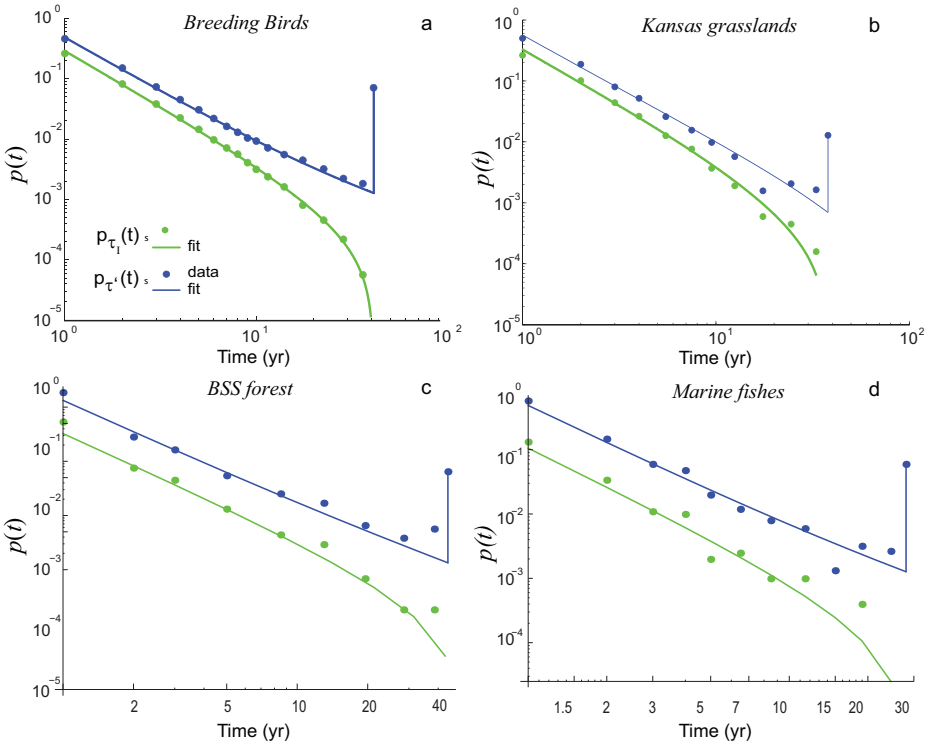

Figure C.4: Comparison between empirical distributions for (a) North American Breeding birds, (b) Kansas grasslands, (c) New Jersey BSS forest, (d) estuarine fish community and the corresponding theoretical SPT pdfs $p(t)$ of τ' (green), τ'' (blue). Filled circles and solid lines show observational distributions and fits, respectively. The spatial scale of analysis is $A = 10,000$ km^2 and $\Delta t_w = 41$ years for (a), A=1 m^2 and $\Delta t_w = 38$ years for (b), A=480 m^2 and $\Delta t_w = 44$ years for (c) and $\Delta t_w = 28$ years for (d) (for details on the analysis of the databases relevant to (a) and (b) see supplementary material in Bertuzzo et al., 2011). The finiteness of the time window imposes a cut-off to $p_{\tau'}(t)$ and an atom of probability in $t = \Delta t_w$ to $p_{\tau''}(t)$, which corresponds to the fraction of species that are always present during the observational time. $p_{\tau_I}(t)$ and $p_{\tau'}(t)$ have been shifted in the log-log plot for clarity.

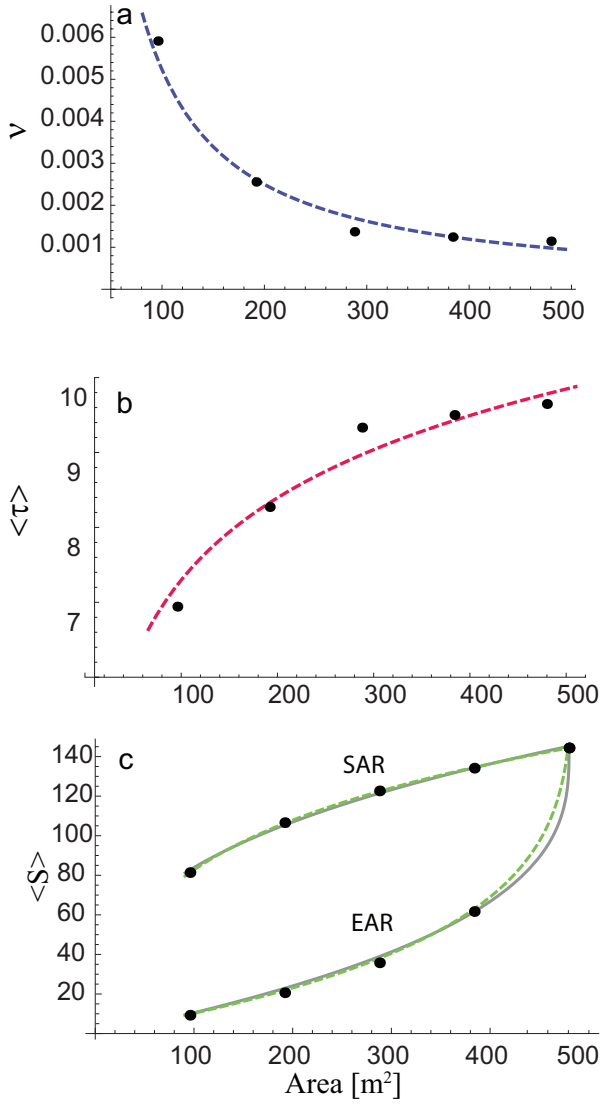

Figure C.5: Comparison between a) diversification rates for different areas (black dots) and the scaling law $\nu \sim A^{-1}$ (dashed blue line); b) mean persistence time for each sample area $\langle \tau(\nu(A), \bar{\alpha}) \rangle$(black dots) calculated using Eq. (3), and logarithmic relation $\tau \sim \ln(A)$ (dashed red line) predicted by the neutral model for the mean field case ($\alpha = 2$); c) empirical SAR and EAR relationships (black points), power law fitting of the SAR and the corresponding EAR (gray continuous line) and the mean field SAR and EAR given by Eqs. (10) and (11) (green dashed).

ecosystem	**A** $[\mathbf{m}^2]$	α	ν
BSS plants	98	1.97	0.0057
BSS plants	196	1.97	0.0024
BSS plants	294	1.96	0.0013
BSS plants	382	1.96	0.0011
BSS plants	480	1.96	0.0010
Hinkley fish	/	1.97 ± 0.06	0.00049 ± 0.00007

Table C.1: Exponents for the Hinkley Point estuarine fish database and for the BSS dataset at every spatial scale of analysis. The values of the exponents are obtained by the simultaneous best fitting of Eqs. (6) and (7) on the empirical SPT distributions. They suggest that both ecosystems are driven by a mean field dynamics. The value of $\bar{\alpha}$ given in the text corresponds to $\bar{\alpha} = (\sum_{i=1}^{5} \alpha_i)/5 = 1.97 \pm \sigma_{\bar{\alpha}}$, where $\sigma^2_{\bar{\alpha}} = \sum_{i=1}^{5} \sigma^2_{\alpha_i}/5 = 0.015$ ($\sigma^2_{\alpha_i}$ is the variance for the $i-$th α exponent from the fit). Values of ν for the BSS plants are obtained by the minimization procedure explained in the text and in Appendix B.